

This is the peer reviewed version of the following article: Auld SKJR, Brand J. Simulated climate change, epidemic size, and host evolution across host–parasite populations. *Glob Change Biol.* 2017;23:5045–5053, which has been published in final form at <https://doi.org/10.1111/gcb.13769>. This article may be used for non-commercial purposes in accordance With Wiley Terms and Conditions for self-archiving.

1 **Simulated climate change, epidemic size and host evolution across host-parasite**
2 **populations**

3 **Authors:** Stuart K.J.R Auld*¹, June Brand¹

4 ¹Biological & Environmental Sciences, University of Stirling, Stirling, United
5 Kingdom

6 *Corresponding author

7 **Emails:** s.k.auld@stir.ac.uk, june.brand@stir.ac.uk

8 Accepted for publication in *Global Change Biology* by Wiley-Blackwell.

9 **Running title:** Climate change and disease eco-evolution

10 **Keywords:** global warming, disease ecology, eco-evolutionary dynamics,
11 mesocosms, parasitism

12 **Article type:** Primary research

13 **Abstract word count:** 162; **Total word count:** 6530.

14 **Figures:** 4 in main text; 3 in supplementary material.

15 **Tables:** 2 in main text; 4 in supplementary material

16 **References:** 56.

17 **Correspondence address:** Room 3A149, Cottrell Building, University of Stirling,
18 Stirling, Stirlingshire, FK9 4LA, UK. **Email:** s.k.auld@stir.ac.uk. **Telephone:** +44
19 (0)1786 467857

20

21

22 **Abstract**

23 Climate change is causing warmer and more variable temperatures as well as physical
24 flux in natural populations, which will affect the ecology and evolution of infectious
25 disease epidemics. Using replicate semi-natural populations of a coevolving
26 freshwater invertebrate-parasite system (host: *Daphnia magna*, parasite: *Pasteuria*
27 *ramosa*), we quantified the effects of ambient temperature and population mixing
28 (physical flux within populations) on epidemic size and population health. Each
29 population was seeded with an identical suite of host genotypes and dose of parasite
30 transmission spores. Biologically reasonable increases in environmental temperature
31 caused larger epidemics, and population mixing reduced overall epidemic size.
32 Mixing also had a detrimental effect on host populations independent of disease.
33 Epidemics drove parasite-mediated selection, leading to a loss of host genetic
34 diversity, and mixed populations experienced greater evolution due to genetic drift
35 over the season. These findings further our understanding of how diversity loss will
36 reduce the host populations' capacity to respond to changes in selection, therefore
37 stymying adaptation to further environmental change.

38

39

40

41 INTRODUCTION

42 The earth's climate is changing, giving rise to warmer temperatures and more variable
43 weather (Coumou & Rahmstorf, 2012). Heat waves, droughts and floods are more
44 common and are driving shifts in the severity and distribution of infectious disease.
45 Warming can increase parasite development rate and transmission stage production
46 (Poulin, 2006), as well as overall transmission rate (Kilpatrick *et al.*, 2008), whereas
47 increased variance in temperature can independently drive shifts in parasite growth
48 and transmission (Murdock *et al.*, 2016). Temperature changes can also differentially
49 affect the phenology of hosts and parasites in such a way to either increase or reduce
50 transmission. For example, warming increases the likelihood and severity of
51 trematode infections in snails, but reduces the likelihood of onward trematode
52 transmission (and thus epidemic size) to the definitive amphibian host (Paull &
53 Johnson, 2014). Physical flux resulting from droughts, floods *etc.* could also have
54 profound effects on disease by increasing contact rates between hosts and parasites
55 and thus parasite transmission rate (May & Anderson, 1979). It is clear that the effects
56 of climate change on infectious diseases are often complex, and can shape disease
57 dynamics in sometimes unpredictable and counter-intuitive ways (Parmesan & Yohe,
58 2003; Lafferty, 2009).

59 By affecting epidemic size, climate change could have profound effects on
60 host populations. Epidemics can reduce population densities in susceptible hosts, and
61 thus drive parasite-mediated selection (Auld *et al.*, 2013) and population genetic
62 change (Duncan & Little, 2007; Thrall *et al.*, 2012). For example, larger epidemics
63 can exert stronger directional selection for increased host resistance, stripping genetic
64 variation from populations (Obbard *et al.*, 2011). Patterns of epidemic size, parasite-

65 mediated selection and host genetic diversity are thus intrinsically linked. This is
66 important, because genetic diversity determines how a host population can respond to
67 subsequent disease epidemics (Altermatt & Ebert, 2008; King & Lively, 2012), as
68 well as other selective pressures. Indeed, genetic diversity is the fuel for adaptation, so
69 low diversity populations are vulnerable to extinction when there is a change in
70 selection pressures (Lande & Shannon, 1996). By influencing epidemic size,
71 environmental variables such as ambient temperature and physical flux are pivotal in
72 shaping eco-evolutionary feedbacks and long-term health in natural populations
73 (Vander Wal *et al.*, 2014).

74 The effects of biotic and abiotic environmental conditions on individual
75 disease phenotypes have been effectively dissected using controlled laboratory
76 experiments in numerous systems (McNew, 1960; Salvaudon *et al.*, 2009; Wolinska
77 & King, 2009; Vale, 2011). However, in order to identify the mechanisms through
78 which climate change shapes the evolution of disease more generally, we must
79 incorporate ecological complexity to determine how these individual phenotypes scale
80 up to the population level. Population-level studies are commonly observational, so
81 the benefit of having a realistic assessment of disease patterns in ecologically complex
82 conditions is often accompanied with the cost of not being able to uncover the
83 mechanisms that drive those patterns. The challenge is to incorporate realistic
84 ecological complexity whilst retaining a degree of experimental control. Semi-natural
85 experimental populations - mesocosms - provide an excellent opportunity to do this
86 (Benton *et al.*, 2007) because they allow natural variation in season, and thus
87 photoperiod and temperature, yet are easily subject to experimental manipulation.

88 Here, we present the results of an outdoor mesocosm experiment designed to
89 test the following hypotheses: that the mean and variance in temperature as well as

90 physical flux (population mixing) affects: (1) the timing and severity of disease
91 epidemics; (2) the strength and consistency of parasite-mediated selection; and (3) the
92 genetic diversity of host populations. We established twenty replicate outdoor
93 mesocosms of the freshwater crustacean, *Daphnia magna* and its sterilizing bacterial
94 parasite, *Pasteuria ramosa*. *Daphnia* have a remarkable reproductive biology that
95 means they can reproduce both sexually and asexually. By propagating *Daphnia*
96 genotypes asexually, we were able to seed each mesocosm with an identical suite of
97 *Daphnia* genotypes as well as spores from the same starting parasite population.
98 Whilst the genetic composition of hosts and parasites was the same across
99 mesocosms, the ambient temperature and level of population mixing varied. This
100 experimental system therefore allowed us to incorporate ecological complexity whilst
101 maintaining control over the genetic composition of the key antagonists.

102

103 **MATERIALS AND METHODS**

104 **Host and parasite organisms**

105 The host, *Daphnia magna* (Straus, 1820), is a freshwater crustacean that inhabits
106 shallow freshwater ponds that are naturally susceptible to temperature fluctuations.
107 The parasite, *Pasteuria ramosa* (Metchnikoff, 1888), is a spore-forming bacterium
108 that sterilizes its hosts. *Daphnia magna* (hereafter: *Daphnia*) and *Pasteuria ramosa*
109 (hereafter: *Pasteuria*) are a naturally coevolving host-parasite system (Decaestecker *et*
110 *al.*, 2007). *Daphnia* commonly encounter *Pasteuria* transmission spores when filter
111 feeding; once inside the host, spores cross the gut epithelium (Duneau *et al.*, 2011;
112 Auld *et al.*, 2012) and proliferate (Auld *et al.*, 2014a), stealing resources that would
113 otherwise be used for host reproduction (Cressler *et al.*, 2014). Millions of *Pasteuria*
114 transmission spores are then released into the environment upon host death (Ebert *et*

115 *al.*, 1996). *Pasteuria* infection is easily diagnosed by eye: infected *Daphnia* have
116 obvious red-brown bacterial growth in their hemolymph, lack developed ovaries or
117 offspring in their brood chamber and sometimes exhibit gigantism (Ebert *et al.*, 1996;
118 Cressler *et al.*, 2014).

119 *Daphnia magna* are cyclically parthenogenetic: they reproduce asexually in
120 the main, but produce males and undergo sexual reproduction when environmental
121 conditions become unfavorable (Hobaek & Larsson, 1990). Host sex results in the
122 production of one or two eggs that are encased in an environmentally resistant
123 envelope called an ephippium. Once ephippia are released by the host, they fall to the
124 sediment and the eggs they contain hatch in later years. We collected three sediment
125 samples from Kaimes Farm, Leitholm, Scottish Borders, UK (2°20'43"W,
126 55°42'15"N) (Auld *et al.*, 2014b) in June 2014. From these sediment samples, we
127 isolated and hatched 21 sexually produced *Daphnia* resting eggs and propagated them
128 clonally by maintaining them under favorable conditions.

129

130 **Experimental setup**

131 We exposed ~20 *Daphnia* from each of the 21 *Daphnia* clonal lines to the original
132 sediment samples and isolated those hosts that became infected with *Pasteuria* (total
133 = 224 infected *Daphnia*, with a minimum of one infection per genotype). Each
134 infected *Daphnia* was individually homogenized and the density of *Pasteuria*
135 transmission spores was determined using a Neubauer (Improved) hemocytometer.
136 We then propagated these spores by exposing 5×10^5 *Pasteuria* spores from each
137 infected *Daphnia* to a further 80 healthy *Daphnia* of the same genotype (the
138 remaining spores were pooled and stored at -20°C). After 35 days, these *Daphnia*

139 were homogenized, pooled and the density of spores was determined. We then
140 performed a second round of propagation. After three rounds of infection (isolation
141 followed by two rounds of propagation), all spore samples were pooled and the total
142 number was determined.

143 Meanwhile, we genotyped each of the 21 *Daphnia* clonal lines using 15
144 microsatellite loci (see *DNA extraction and microsatellite genotyping*), and selected
145 the 12 most dissimilar multilocus genotypes for the mesocosm experiment. Replicate
146 lines of each *Daphnia* of the 12 genotypes were maintained in a state of clonal
147 reproduction for three generations to reduce variation due to maternal effects. There
148 were five replicates per genotype; each replicate consisted of five *Daphnia* kept in
149 200mL of artificial medium ((Klüttgen *et al.*, 1994) modified using 5% of the
150 recommended SeO₂ concentration (Ebert *et al.*, 1998)). Replicate jars were fed 5.0
151 ABS of *Chlorella vulgaris* algal cells per day (ABS is the optical absorbance of
152 650nm white light by the *Chlorella* culture). *Daphnia* medium was changed three
153 times per week and three days prior to the start of the mesocosm experiment. On the
154 day that the mesocosm experiment commenced, 1-3 day old offspring were pooled
155 according to host genotype. Ten offspring per *Daphnia* genotype were randomly
156 allocated to each of the 20 mesocosms (giving a total of 120 *Daphnia* per mesocosm).

157

158 **Mesocosm experiment**

159 Each mesocosm consisted of a 0.65m tall 1000 Liter PVC tank. Mesocosms were dug
160 into the ground during July and August and were lined with ~10cm of topsoil; they
161 were dug in to differing depths (0-0.64m) in order to promote variation in water
162 temperature. The mesocosms were allowed to naturally fill with rainwater over an

163 eight month period prior to the experiment. During the experiment, half of the
164 mesocosms experienced a weekly population mixing (physical flux) treatment, where
165 mixed mesocosms were stirred once across the middle and once around the
166 circumference with a 0.35m² paddle submerged halfway into the mesocosm (the
167 exception to this was on the first day of the experiment, when all mesocosms
168 experienced the mixing treatment to ensure hosts and parasites were distributed
169 throughout the mesocosms). Deeper mesocosms had lower mean temperatures over
170 the season (Spearman's Rank correlation: $r_s = -0.98$, $p < 0.0001$). Mixing and
171 temperature treatments were haphazardly distributed across the mesocosms, and mean
172 temperature was not different between mixing treatments (mean temperature: $t =$
173 0.04, $DF = 17.87$, $p = 0.97$).

174 The experiment began on the 2nd April 2015 (Julian day 98), when 120
175 *Daphnia* (10 *Daphnia* x 12 genotypes) and 1×10^8 *Pasteuria* spores were added to
176 each of the 20 mesocosms. Between the 2nd April and the 17th November 2015, we
177 measured the temperature (°C, using an Aquaread AP-5000 probe; Aquaread,
178 Broadstairs, Kent, UK) and depth of each mesocosm (m) on a weekly basis. After
179 allowing a two week period for the *Daphnia* to establish (*i.e.*, from 16th April 2015),
180 we measured the density of various *Daphnia* life stages in each mesocosm each week
181 (juveniles, healthy adults, *Pasteuria*-infected adults). We did this by passing a 0.048
182 m² pond net across the diameter of the mesocosm (1.51 m) and counting the resulting
183 *Daphnia*. If there were fewer than 100 *Daphnia* from the net sweep, we took a second
184 sweep of the mesocosm. All *Daphnia* were returned to their respective mesocosms
185 following population counts. Twenty-thirty *Daphnia* were sampled from each
186 mesocosm for genotyping on two occasions during the season: once before peak
187 epidemic (24th May 2015; Julian day 144) and once after peak epidemic (17th

188 November 2015; Julian Day 321). It is important to note that due to low population
189 densities, we were only able to sample 16 of the 20 mesocosms (10 unmixed, 6
190 mixed) for population genetic analysis.

191

192 **DNA extraction and microsatellite genotyping**

193 Microsatellite genotyping was used to both identify the twelve unique multilocus
194 *Daphnia* genotypes to follow their frequencies over the season during the experiment.
195 We extracted genomic DNA from individual *Daphnia* using NucleoSpin Tissue XS
196 (Macherey Nagel) following the manufacturers protocols. *Daphnia* were genotyped at
197 15 microsatellite markers assembled in two multiplexes for PCR reactions ((Jansen *et*
198 *al.*, 2011); see Table S1 for a list of marker loci). For each reaction, forward primers
199 were fluorescently labelled with different dyes, thus allowing us to identify four
200 distinct loci. Multiplex PCR reactions were 10 μ L in volume and consisted of 1 μ L
201 DNA extract, 5 μ L of, 2x Type-it Multiplex PCR Mastermix (Qiagen), 3 μ L Nuclease
202 Free H₂O and 1 μ L of 10x primer mix solution (2 μ M of each primer). PCR Reactions
203 were performed using the following protocol: Taq activation step at 95°C for 15
204 mins, followed by 30 cycles of 94°C for 30 secs, 57°C for 90 secs, 72°C for 90secs,
205 72 °C for 90 secs and a final extension at 60°C for 30 mins. PCR products were
206 analyzed using an ABI 3730XL DNA Analyzer with the GeneScan-500 LIZ size
207 standard (Applied Biosystems). Allele sizes were scored, using Geneous v9.0.5
208 (Biomatters) and validated manually.

209

210 **Analysis**

211 Data were analyzed using R 3.0.2. Data and code will be archived on Dryad upon
212 acceptance of the manuscript. We analyzed how parasite prevalence varied over time
213 using a Generalized Additive Model (GAM) with a binomial error distribution. GAMs
214 fit non-parametric smoothing functions to covariates in a model (in this case, Julian
215 Day), and allow comparisons between trajectories of the response variable with
216 respect to other factors without the need to fit particular functions to the data. We
217 fitted four GAMs to the parasite prevalence data: all models included the volume of
218 water sampled as a covariate and Julian Day as a non-parametric smoother; physical
219 flux treatment and mean mesocosm temperature were either fitted as fixed effects or
220 as modifiers to the Julian Day smoother function in the other three models (see Table
221 1). We then compared the fits of the models using AIC in order to determine if the
222 relationship between parasite prevalence and Julian Day varied according to mixing
223 treatment, mean mesocosm temperature or both (Table 1). Since parasite prevalence
224 depends on both the numbers of healthy and infected hosts, we fitted separate sets of
225 GAMs with negative binomial errors to counts of infected and healthy adults in order
226 to determine if mixing treatment or mean mesocosm temperature differentially
227 affected hosts from different infection classes over time (see Table S2, S3). We also
228 tested the relationship between epidemic size and severity. We did this by fitting a
229 Generalized Linear Mixed Effects Model (GLMM) with binomial errors to data for
230 the proportion of juveniles in the host population (a key measure of population of
231 health given that the parasite sterilizes its host), with parasite prevalence and volume
232 of water samples as fixed effects and host population and sample date fitted as
233 random effects.

234 Second, we calculated the overall epidemic size for each mesocosm. This was
235 done by integrating the area under the time series of empirically determined

236 prevalence for each mesocosm. We then tested how mean and variance in
237 temperatures, and mixing treatment, affected overall epidemic size. This was done by
238 fitting a linear model (LM) to the epidemic size data with mixing treatment, mean
239 temperature, variance in temperature and all two-way interactions as fixed effects.

240 Third, we analyzed how host genotype frequencies changed over the course of
241 the season. We analyzed mixed and unmixed mesocosms separately, using two LMs.
242 For each LM, we fitted multilocus genotype identity and sampling time (start, pre-
243 epidemic or post-epidemic) as fixed factors. We then performed *post hoc* tests to
244 examine how genotype frequencies changed between the start and pre-epidemic
245 sampling and between the pre-epidemic and post-epidemic sampling. In order to
246 assess the level of genetic drift, we determined the level of among-population
247 differentiation within mixing treatments and over time. We did this by calculating F_{ST}
248 values for genotype data collected from mixed and unmixed mesocosms both pre- and
249 post-epidemic. F_{ST} is a reliable measure of drift here, because we can be confident
250 that standing host population consists of only asexually produced progeny (sexually
251 produced eggs drop to the sediment and hatch in future years, and we found no
252 recombinant genotypes in individuals collected throughout the experiment). Finally,
253 we examined how host genotypic evenness (a measure of genetic diversity (Smith &
254 Wilson, 1996)) covaried with mesocosm epidemic size and mixing treatment. We
255 analyzed evenness data using a LM, with epidemic size, mixing treatment, sample
256 time (pre- or post-epidemic) and all two-way interactions fitted as fixed factors.

257

258 **RESULTS**

259 **Temperature and population mixing determine epidemic size**

260 *Pasteuria* –infected hosts were observed from mid-May until mid-November
261 (between Julian days 106 and 321). The timing and magnitude of *Pasteuria* epidemics
262 varied across populations, as did various other environmental variables. Populations
263 typically experienced a small peak in parasite prevalence in early June (~ day 160)
264 and a much larger peak late July-early August (~day 210-250; Fig. 1). Both
265 prevalence peaks were higher in unmixed than in mixed populations and the second
266 peak was earlier and larger in warmer populations than in cooler ones (Fig. 1; Table
267 1). The shape of the relationship between parasite prevalence and time depended on
268 both mixing treatment and mean temperature of the population (Fig. 1; Table 1).
269 Further analysis revealed that warmer populations had higher numbers of infected
270 hosts, but not healthy hosts, and that unmixed populations had higher numbers of both
271 healthy and infected hosts than mixed populations (Table S2, S3, Fig. S1, S2). The
272 proportion of the host population that consisted of juveniles was negatively associated
273 with parasite prevalence (Fig. S3; GLMM: $z = 5.47$, $P < 0.0001$), demonstrating the
274 impact of this sterilizing parasite on host populations. Overall epidemic size
275 (measured as parasite prevalence integrated over time) was larger in populations
276 where mean temperature was high (Fig. 2A; LM: $F_{1,16} = 8.70$, $P = 0.009$), variance in
277 temperature was low (Fig. 2B; LM: $F_{1,16} = 4.52$, $P = 0.049$) and in populations that
278 were unmixed (Fig. 2C; LM: $F_{1,16} = 8.81$, $P = 0.009$).

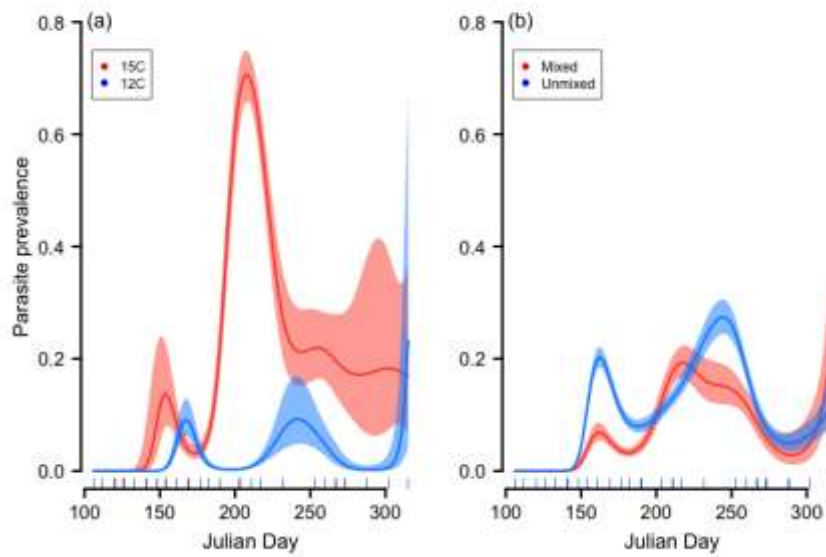


Figure 1. Parasite prevalence over time across 20 replicate mesocosm populations according to (a) mean population temperature and (b) population mixing treatment. The lines represent proportion of hosts infected as predicted by a generalized additive model (GAM; see Table 1) at ambient temperatures of 12°C and 15°C or for each mixing treatment (temperature was fitted as a covariate, but model predictions for two temperatures are shown for clarity). The shaded areas denote 95% confidence intervals (CIs).

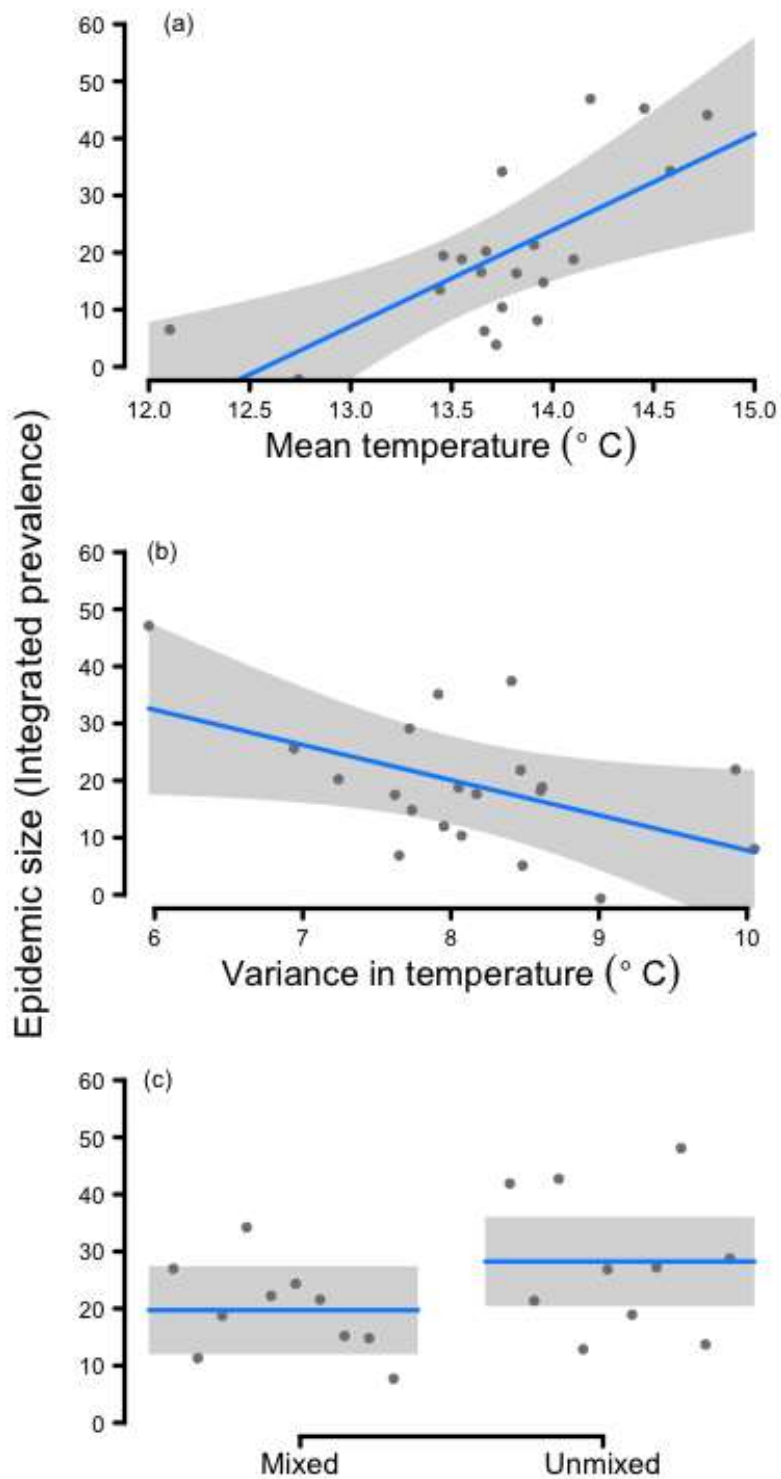


Figure 2. Relationship between epidemic size and (a) mean population temperature, (b) variance in population temperature, and (c) population mixing treatment. Lines show epidemic sizes as predicted by a linear model, shaded areas denote 95% CIs.

Table 1. **A** Generalized Additive Models fitted to parasite prevalence data. In all four models, sweep volume is fitted as a fixed effect and Julian Day as a non-parametric smoother; mean mesocosm temperature and mixing treatment are fitted as either fixed effects or as modifiers of the Julian Day smoother function. The model that best explains variation in parasite prevalence (here, the model with the lowest AIC value, model 4) is highlighted in bold. **B** Summary analysis for model 4. eDF is the estimated degrees of freedom.

A Model selection					
Model	Parametric	Smoother	Deviance explained %	AIC	
1	Sweep Vol; Mean Temp; Mixing	Julian Day	40.3	4754	
2	Sweep Vol; Mean Temp	Julian Day by Mixing	40.4	4748	
3	Sweep Vol; Mixing	Julian Day by Mean Temp	42.1	4647	
4	Sweep Vol	Julian Day by Mixing; Julian Day by Mean Temp	45.6	4428	

B Model 4 results					
Response	Parametric/Smoother	Term	DF (eDF)	χ^2	<i>P</i>
Parasite prevalence	Parametric	Sweep Vol	1	18.82	<0.0001
	Smoother	Julian Day by Mean Temp	9.77	477	<0.0001
	Smoother	Julian Day, Mixed	8.55	210.6	<0.0001
	Smoother	Julian Day, Unmixed	8.08	224.6	<0.0001

279

280 **Epidemic size and population mixing shape host evolution**

281 The relative frequencies of host genotypes changed over the course of the season, and
 282 the nature of this change clearly depended on both epidemic size and mixing
 283 treatment (Fig. 3). In unmixed mesocosms, genotype frequencies depended on an
 284 interaction between the identity of the genotype and the time of sampling (*i.e.*,
 285 whether the hosts were sampled at the start of the experiment, before the epidemic or
 286 after the epidemic. Fig. 4, LM: $F_{22,324} = 2.36$, $P = 0.0007$). *Post hoc* analysis revealed

287 that in unmixed mesocosms, genotype frequencies did not significantly change
288 between the start of the experiment and when the pre-epidemic samples were taken
289 (Tukey test: difference = -0.10, $P = 0.17$), but did change between the pre-epidemic
290 and post-epidemic sampling (Tukey test: difference = -0.18, $P = 0.008$). In mixed
291 mesocosms, genotype frequencies also depended on an interaction between the
292 identity of the genotype and the time of sampling (Fig. 3, LM: $F_{22,180} = 1.72$, $P =$
293 0.030). However, *post hoc* tests showed a significant change in genotype frequencies
294 between the start of the experiment and pre-epidemic sampling (Tukey test: difference
295 = -0.21, $P = 0.032$), but no difference between the pre-epidemic and post-epidemic
296 sampling (Tukey test: difference = -0.17, $P = 0.108$). Population genetic
297 differentiation (a measure of genetic drift) was relatively low in unmixed mesocosms
298 both before peak epidemic ($F_{ST} = 0.09$) and after peak epidemic ($F_{ST} = 0.10$) when
299 compared to wild populations of a much larger size (Vanoverbeke *et al.*, 2007). In
300 mixed mesocosms, population genetic differentiation was higher before peak
301 epidemic ($F_{ST} = 0.12$) and increased towards the end of the season once the epidemic
302 was over ($F_{ST} = 0.20$).
303

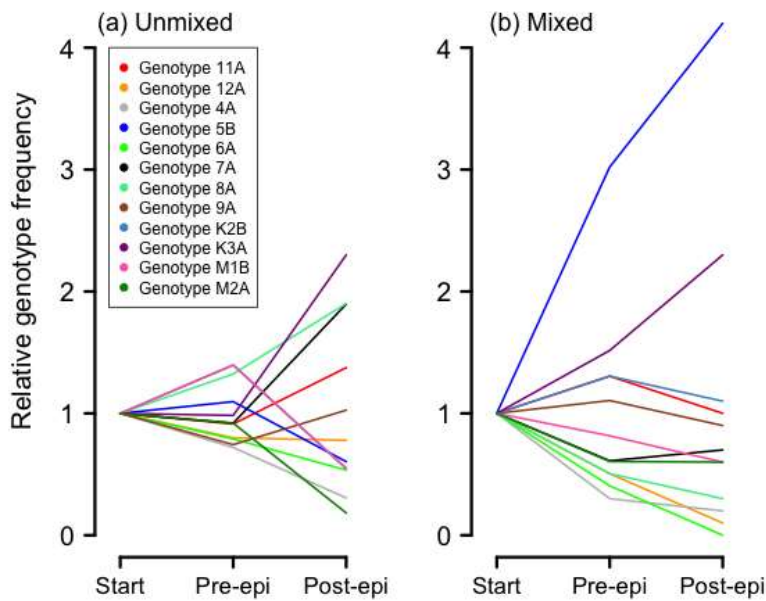


Figure 3. The relative frequencies of each genotype over time in (a) unmixed and (b) mixed populations. There are three sampling points: Start is the beginning of the experiment, when all genotypes were at the same frequency; Pre-epi was on May 24th 2015, before epidemics had peaked; and Post-epi was on November 17th 2015, after epidemics had peaked.

304

305 The relationship between genotypic evenness (a measure of host diversity) and
 306 epidemic size depended on whether samples were collected before or after the
 307 epidemic (Fig. 4, Table 2), where large epidemics were associated with low genotypic
 308 evenness in samples collected after the epidemic had peaked (but not in samples
 309 collected before peak epidemic). Genotypic evenness also depended on an interaction
 310 between mixing treatment and sample time (Fig 4, Table 2): unmixed mesocosms had
 311 higher genotypic evenness, especially in pre-epidemic samples.

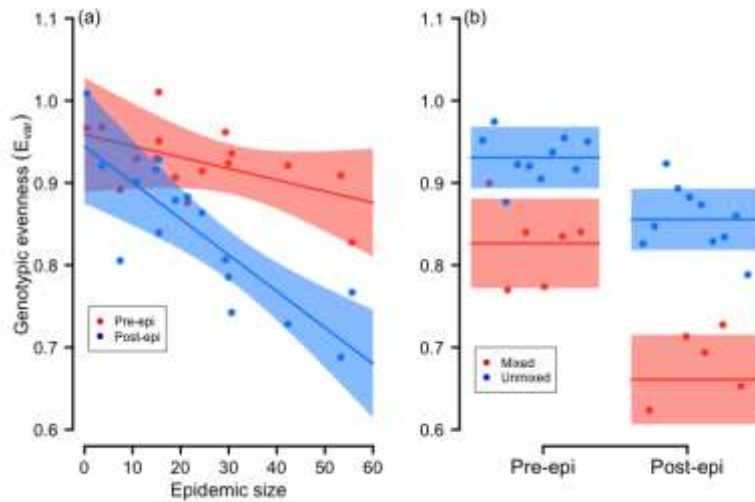


Figure 4. Relationship between host genotypic evenness and (a) epidemic size for pre-epidemic and post-epidemic samples, and (b) time of population sampling for mixed and unmixed populations. Lines show epidemic sizes as predicted by a linear model, shaded areas denote 95% CIs.

312

313 Table 2. Linear model testing effects of epidemic size, population mixing and
 314 sampling time (start, pre-epidemic, post-epidemic) on host genotypic evenness (E_{var} , a
 315 measure of host diversity)

Genotypic Evenness (E_{var})	DF	SS	F	P
Epidemic size (Epi)	1	0.036	16.77	0.0004
Mixing treatment (Mix)	1	0.113	52.62	<0.0001
Sampling time (Samp)	1	0.113	52.44	<0.0001
Epi x Mix	1	0.001	0.37	0.55
Epi x Samp	1	0.011	5.16	0.032
Mixed x Samp	1	0.009	4.32	0.048
Error	25	0.054		

316

317 DISCUSSION

318 Much of our understanding of how climate change affects disease either comes from
 319 controlled laboratory experiments, where the environmental effects can be effectively
 320 dissected but ecological realism is lacking, or from observational studies of
 321 populations, where ecological complexity can mask the drivers of variation in disease.

322 Semi-natural populations provide an excellent opportunity to manipulate
323 environmental conditions while embracing ecological realism (Benton *et al.*, 2007),
324 but see also (Paull & Johnson, 2014). We found that twenty *Daphnia* populations -
325 each consisting of an identical suite of twelve genotypes - suffered very different
326 epidemics of the sterilizing parasite *Pasteuria ramosa* depending on the temperature
327 and mixing treatments they experienced. However, whilst epidemics differed among
328 mesocosm populations, they were similar to natural epidemics in wild populations in
329 that they occurred in the summer and ended in the winter. Both the timing and
330 magnitude of epidemics and the strength of parasite-mediated selection was
331 dependent on mean temperature, temperature variability and population mixing.
332 Furthermore, the mode and tempo of host evolution, and thus the genetic diversity of
333 host populations, was shaped by both epidemic size and mixing treatment.

334 In numerous host-parasite systems, warmer temperatures are associated with
335 increased parasite transmission, within-host growth rates, or both (LaPointe *et al.*,
336 2010; Alonso *et al.*, 2011; Baker-Austin *et al.*, 2013; Burge *et al.*, 2013; Elderd &
337 Reilly, 2014), though see also (Raffel *et al.*, 2013). Laboratory experiments using the
338 *Daphnia-Pasteuria* system demonstrated increased likelihood of infection, higher
339 parasite burdens and increased host mortality rates when hosts were incubated at 20°C
340 than at 15°C (Vale *et al.*, 2008; Vale & Little, 2009). However, those studies also
341 demonstrated that warming led to increased fecundity in uninfected *Daphnia* (as is
342 common in numerous organisms: Huey & Berrigan, 2001; Hochachka & Somero,
343 2016). This raises the question of whether the costs of infection are mitigated by the
344 benefits of increased fitness in uninfected hosts in natural populations. We found that
345 even small increases in ambient temperature (3°C) were associated with increased
346 overall epidemic size. We also found that over the course of the season, warmer

347 mesocosms had greater numbers of juveniles and infected adults, but similar numbers
348 of healthy adults. High prevalence of this sterilizing parasite was, however, associated
349 with a low proportion of juveniles in the host population. Our data therefore suggest
350 that any warming-induced increase in reproduction in healthy hosts served to fuel the
351 epidemic more than growth of the healthy host population.

352 It is not just mean temperature that is important for disease dynamics;
353 temperature variability also plays a major role. Daily temperature variation was found
354 to be negatively associated with the likelihood of the Dengue virus successfully
355 infecting its *Anopheles gambiae* (mosquito) hosts (Lambrechts *et al.*, 2011), and the
356 *Holospora undulata* bacterium infecting its *Paramecium caudatum* hosts (Duncan *et*
357 *al.*, 2011). Whereas, rapid temperature fluctuations increased the likelihood that the
358 fungus *Batrachochytrium dendrobatidis* successfully infected its *Osteopilus*
359 *septentrionalis* (frog) hosts (Raffel *et al.*, 2013) and also fostered greater *B.*
360 *dendrobatidis* growth rate on *Notophthalmus viridescens* (newt) hosts (Raffel *et al.*,
361 2015). Although we did not measure daily temperature fluctuation, we did find that
362 increased weekly temperature variability was associated with smaller *Pasteuria*
363 epidemics. It is unclear exactly how temperature variability limits epidemics in this
364 host-parasite system. However, parasite ability to attach to hosts is very temperature
365 sensitive in the related bacterium, *Pasteuria penetrans*, a parasite of nematodes: a
366 7.5°C deviation from thermal optimum leads to a 15% reduction in *P. penetrans*
367 attachment to the nematode cuticle (Freitas *et al.*, 1997), suggesting parasite
368 attachment should be the focus of future study on how temperature variability affects
369 infection in the *Daphnia magna*-*Pasteuria ramosa* system.

370 In addition to shifts in temperature, changing weather has given rise to

371 increased physical flux in the form of storms and floods. Such flux is known to cause
372 increased mixing in populations and nutrient upwelling (Walker, 1991), with the
373 potential to increase host contact rate with parasite transmission stages and thus
374 epidemic size (May & Anderson, 1979). Based on this, one might expect mixing to
375 lead to larger epidemics, though we found no evidence for this. Contrary to
376 expectations, we found that mixed mesocosms suffered smaller epidemics. It is,
377 however, important to note that population size was universally lower in mixed than
378 in unmixed mesocosms, perhaps because sediment upwelling reduced the efficiency
379 at which *Daphnia* filtered food from the water, thus leading to a lower carrying
380 capacity. So if there were any increases in parasite infection rates due to higher host-
381 parasite contact rate, they were outweighed by negative effects on host reproductive
382 rate.

383 Given that each mesocosm was seeded with identical suites of host genotypes
384 that reproduced asexually throughout the season, we were able to test whether any
385 emergent patterns of selection were shaped by environmental variation and quantify
386 the genetic drift in host populations. Directional selection would favor the same
387 subset of host genotypes across populations, whereas if genetic drift was the principal
388 driver of host evolution, we would observe relatively high among-population genetic
389 differentiation (Vanoverbeke *et al.*, 2007; Vanoverbeke & De Meester, 2010). In
390 unmixed mesocosms, we found that the frequencies of each genotype changed over
391 the course of the season, and the nature of this change depended on the identity of the
392 genotype. Importantly, there was no significant change in genotype frequencies
393 between the start of the experiment and the sample taken before the peak epidemic,
394 but there was a significant change in genotype frequencies between the pre-epidemic
395 and post-epidemic sampling. Among unmixed mesocosms, population genetic

396 differentiation was low (given the small size of the populations: Vanoverbeke *et al.*,
397 2007) and changed minimally over the course of the season. A strong signal of
398 parasite-mediated selection was therefore discernible over and above drift, supporting
399 disease epidemics as the principal driver of host evolution in unmixed mesocosms.

400 Mixed mesocosms showed a different pattern. Whilst the direction of change
401 in genotype frequencies also depended on the identity of the genotype in mixed
402 mesocosms, the significant changes occurred before the peak epidemic. Furthermore,
403 the two host genotypes that increased most in frequency (5B and K3A) were
404 comparatively susceptible to the parasite but had the highest reproductive rates (S.
405 Auld unpublished data). These results are consistent with our epidemiological data,
406 and suggest that mixing exerts strong selection for high fecundity in the host
407 population and that parasite epidemics play a less important role on host evolution
408 than in unmixed mesocosms. On the other hand, population differentiation increased
409 over the course of the season in mixed mesocosms, suggesting that mixing led to a
410 bottleneck that left the host population particularly vulnerable to genetic drift.

411 We sought to test if parasite-mediated selection maintained host genetic
412 diversity (Wolinska & Spaak, 2009) or depleted it by driving selective sweeps
413 (Obbard *et al.*, 2011). Host genotypic evenness – a key measure of population genetic
414 diversity - was negatively associated with epidemic size, particularly in samples
415 collected after peak epidemic. This provides compelling evidence that parasite
416 epidemics apply strong directional selection on host populations. Mixed mesocosms
417 also had lower host genotypic evenness than unmixed populations; once again, this
418 effect was stronger for samples collected after the peak epidemic, and points towards
419 the mixing treatment stripping out host genetic diversity over time. How could this

420 affect the health of populations in the long-term? Selection for increased host
421 resistance could lead to smaller or less severe epidemics in future years. If so, one
422 would expect mesocosms that suffered the largest epidemics in this season to suffer
423 smaller epidemics in the following year. However, this relies on the assumption that
424 host genes that confer resistance to current parasites also confer resistance to future
425 parasites (this is sometimes, though not always the case in this system: (Little &
426 Ebert, 2001; Auld *et al.* 2016). In any case, host populations with low genetic
427 diversity are commonly prone to the spread of severe epidemics because disease
428 transmission is more likely to be successful when hosts are genetically similar
429 (Anderson *et al.*, 1986; King & Lively, 2012). Moreover, a decline in genetic
430 diversity reduces a population's capacity to respond to further selection more
431 generally, because diversity is the currency with which a population pays for
432 adaptation (Lande & Shannon, 1996). Therefore, the low diversity populations in
433 mixed mesocosms are still much more vulnerable to extinction, despite suffering
434 smaller parasite epidemics.

435

436 **STATEMENT OF AUTHORSHIP**

437 SKJRA designed the study, SKJRA and JB collected the data, SKJRA analyzed the
438 data and wrote the first draft of the manuscript, and both authors approved the final
439 version of the manuscript.

440 **DATA ACCESSIBILITY STATEMENT**

441 All data and code will be archived with Dryad upon acceptance of the manuscript.

442 **ACKNOWLEDGEMENTS**

443 This project was funded by a NERC Independent Research Fellowship to SKJRA
444 (NE/L011549/1). We thank three anonymous reviewers for constructive comments.

445 **REFERENCES**

446 Alonso D, Bouma MJ, Pascual M (2011) Epidemic malaria and warmer temperatures
447 in recent decades in an East African highland. *Proceedings of the Royal Society*
448 *B: Biological Sciences*, **278**, 1661–1669.

449 Altermatt F, Ebert D (2008) Genetic diversity of *Daphnia magna* populations
450 enhances resistance to parasites. *Ecology Letters*, **11**, 918–928.

451 Anderson RM, May RM, Joysey K et al. (1986) The invasion, persistence and spread
452 of infectious diseases within animal and plant communities. *Philosophical*
453 *Transactions of the Royal Society B: Biological Sciences*, **314**, 533–570.

454 Auld SKJR, Graham AL, Wilson PJ, Little TJ (2012) Elevated haemocyte number is
455 associated with infection and low fitness potential in wild *Daphnia magna*.
456 *Functional Ecology*, **26**, 434–440.

457 Auld SKJR, Hall SR, Ochs JH, Sebastian M, Duffy MA (2014a) Predators and
458 patterns of within-host growth can mediate both among-host competition and
459 evolution of transmission potential of parasites*. *American Naturalist*, **184**, S77-
460 S90.

461 Auld SKJR, Penczykowski RM, Housley Ochs J, Grippi DC, Hall SR, Duffy MA
462 (2013) Variation in costs of parasite resistance among natural host populations.
463 *Journal of Evolutionary Biology*, **26**, 2479–2486.

464 Auld SKJR, Tinkler, SK, Tinsley, MC (2016) Sex as a strategy against rapidly
465 evolving parasites. *Proceedings of the Royal Society B*, **283**, 20162226.

466 Auld SKJR, Wilson PJ, Little TJ (2014b) Rapid change in parasite infection traits
467 over the course of an epidemic in a wild host–parasite population. *Oikos*, **123**,

468 232–238.

469 Baker-Austin C, Trinanes JA, Taylor NGH, Hartnell R, Siitonen A, Martinez-Urtaza J
470 (2013) Emerging *Vibrio* risk at high latitudes in response to ocean warming.
471 *Nature Climate Change*, **3**, 73–77.

472 Beisner BE (2001) Herbivory in variable environments: an experimental test of the
473 effects of vertical mixing and *Daphnia* on phytoplankton community structure.
474 *Canadian Journal of Fisheries and Aquatic Sciences*, **58**, 1371–1379.

475 Benton TG, Solan M, Travis JMJ, Sait SM (2007) Microcosm experiments can inform
476 global ecological problems. *Trends in Ecology & Evolution*, **22**, 516–521.

477 Burge CA, Kim CJS, Lyles JM, Harvell CD (2013) Oceans and human health: The
478 ecology of marine opportunists. *Microbial Ecology*, **65**, 869–879.

479 Coumou D, Rahmstorf S (2012) A decade of weather extremes. *Nature Climate
480 Change*, **2**, 491–496.

481 Cressler CE, Nelson WA, Day T, McCauley E (2014) Starvation reveals the cause of
482 infection-induced castration and gigantism. *Proceedings of the Royal Society B:
483 Biological Sciences*, **281**, 20141087.

484 Decaestecker E, Gaba S, Raeymaekers JAM, Stoks R, Van Kerckhoven L, Ebert D,
485 De Meester L (2007) Host-parasite "Red Queen" dynamics archived in pond
486 sediment. *Nature*, **450**, 870–873.

487 Duncan AB, Little TJ (2007) Parasite-driven genetic change in a natural population of
488 *Daphnia*. *Evolution*, **61**, 796–803.

489 Duncan AB, Fellous S, Kaltz O (2011) Temporal variation in temperature determines
490 disease spread and maintenance in *Paramecium* microcosm populations.
491 *Proceedings of the Royal Society B: Biological Sciences*, rspb20110287.

492 Duneau D, Luijckx P, Ben Ami F, Laforsch C, Ebert D (2011) Resolving the infection

493 process reveals striking differences in the contribution of environment, genetics
494 and phylogeny to host-parasite interactions. *BMC Biology*, **9**, 11.

495 Ebert D, Rainey P, Embley TM, Scholz D (1996) Development, life cycle,
496 ultrastructure and phylogenetic position of *Pasteuria ramosa* Metchnikoff 1888:
497 Rediscovery of an obligate endoparasite of *Daphnia magna* Straus. *Philosophical
498 Transactions of the Royal Society B: Biological Sciences*, **351**, 1689–1701.

499 Ebert D, Zschokke-Rohringer CD, Carius HJ (1998) Within–and between–population
500 variation for resistance of *Daphnia magna* to the bacterial endoparasite *Pasteuria
501 ramosa*. *Proceedings of the Royal Society B: Biological Sciences*, **265**, 2127–
502 2134.

503 Elderd BD, Reilly JR (2014) Warmer temperatures increase disease transmission and
504 outbreak intensity in a host-pathogen system. *Journal of Animal Ecology*, **83**,
505 838–849.

506 Freitas LG, Mitchell DJ, Dickson DW (1997) Temperature Effects on the Attachment
507 of *Pasteuria penetrans* Endospores to *Meloidogyne arenaria* Race 1. *Journal of
508 Nematology*, **29**, 547-555.

509 Hobaek A, Larsson P (1990) Sex determination in *Daphnia magna*. *Ecology*, **71**,
510 2255-2268.

511 Hochachka PW, Somero GN (2016) *Hochachka, P.W. and Somero, G.N.:*
512 *Biochemical Adaptation (eBook, Paperback and Hardcover)*.

513 Huey RB, Berrigan D (2001) Temperature, demography, and ectotherm fitness.
514 *American Naturalist*, **158**, 204–210.

515 Jansen B, Geldof S, De Meester L (2011) Isolation and characterization of
516 microsatellite markers in the waterflea *Daphnia magna*. *Molecular Ecology
517 Resources*.

518 Kilpatrick AM, Meola MA, Moudy RM, Kramer LD (2008) Temperature, viral
519 genetics, and the transmission of West Nile virus by *Culex pipiens* mosquitoes.
520 *PLOS Pathogens*, **4**, e1000092.

521 King KC, Lively CM (2012) Does genetic diversity limit disease spread in natural
522 host populations? *Heredity*, **109**, 199–203.

523 Klüttgen B, Dülmer U, Engels M, Ratte HT (1994) ADaM, an artificial freshwater for
524 the culture of zooplankton. *Water research*, **28**, 743–746.

525 Lafferty KD (2009) Calling for an ecological approach to studying climate change
526 and infectious diseases. *Ecology*, **90**, 932–933.

527 Lambrechts L, Paaijmans KP, Fansiri T, Carrington LB, Kramer LD, Thomas MB,
528 Scott TW (2011) Impact of daily temperature fluctuations on dengue virus
529 transmission by *Aedes aegypti*. *Proceedings of the National Academy of Sciences*,
530 **108**, 7460–7465.

531 Lande R, Shannon S (1996) The role of genetic variation in adaptation and population
532 persistence in a changing environment. *Evolution*, **50**, 434–437.

533 LaPointe DA, Goff ML, Atkinson CT (2010) Thermal constraints to the sporogonic
534 development and altitudinal distribution of avian malaria *Plasmodium relictum* in
535 Hawai'i. *Journal of Parasitology*, **96**, 318–324.

536 Levine SN, Zehrer RF, Burns CW (2005) Impact of resuspended sediment on
537 zooplankton feeding in Lake Waiholo, New Zealand. *Freshwater Biology*, **50**,
538 1515–1536.

539 Little TJ, Ebert D (2001) Temporal patterns of genetic variation for resistance and
540 infectivity in a *Daphnia*-microparasite system. *Evolution*, **55**, 1146–1152.

541 May RM, Anderson RM (1979) Population biology of infectious diseases: Part II.
542 *Nature*, **280**, 455–461.

543 McNew GL (1960) *McNew: The nature, origin, and evolution of parasitism*. Plant
544 pathology: an advanced treatise.

545 Murdock CC, Sternberg ED, Thomas MB (2016) Malaria transmission potential could
546 be reduced with current and future climate change. *Scientific Reports*, **6**, 27771.

547 Obbard DJ, Jiggins FM, Bradshaw NJ, Little TJ (2011) Recent and recurrent selective
548 sweeps of the antiviral RNAi gene *Argonaute-2* in three species of *Drosophila*.
549 *Molecular Biology and Evolution*, **28**, 1043–1056.

550 Parmesan C, Yohe G (2003) A globally coherent fingerprint of climate change
551 impacts across natural systems. *Nature*, **421**, 37–42.

552 Paull SH, Johnson PTJ (2014) Experimental warming drives a seasonal shift in the
553 timing of host- parasite dynamics with consequences for disease risk. *Ecology*
554 *Letters*, **17**, 445–453.

555 Poulin R (2006) Global warming and temperature-mediated increases in cercarial
556 emergence in trematode parasites. *Parasitology*, **132**, 143–151.

557 Raffel TR, Halstead NT, McMahon TA, Davis AK, Rohr JR (2015) Temperature
558 variability and moisture synergistically interact to exacerbate an epizootic disease.
559 *Proceedings of the Royal Society B: Biological Sciences*, **282**, 20142039.

560 Raffel TR, Romansic JM, Halstead NT, McMahon TA, Venesky MD, Rohr JR (2013)
561 Disease and thermal acclimation in a more variable and unpredictable climate.
562 *Nature Climate Change*, **3**, 146–151.

563 Salvaudon L, Héraudet V, Shykoff JA (2009) Parasite-host fitness trade-offs change
564 with parasite identity: genotype-specific interactions in a plant-pathogen system.
565 *Evolution*, **59**, 2518-2524.

566 Smith B, Wilson JB (1996) A Consumer's Guide to Evenness Indices. *Oikos*, **76**, 70-
567 82.

568 Thrall PH, Laine A-L, Ravensdale M, Nemri A, Dodds PN, Barrett LG, Burdon JJ
569 (2012) Rapid genetic change underpins antagonistic coevolution in a natural
570 host- pathogen metapopulation. *Ecology Letters*, **15**, 425–435.

571 Vale PF, Little TJ (2009) Measuring parasite fitness under genetic and thermal
572 variation. *Heredity*, **103**, 102–109.

573 Vale PF, Stjernman M, Little TJ (2008) Temperature- dependent costs of parasitism
574 and maintenance of polymorphism under genotype- by- environment
575 interactions. *Journal of Evolutionary Biology*, **21**, 1418–1427.

576 Vale PF, Wilson AJ, Best A, Boots M, Little TJ (2011) Epidemiological, evolutionary
577 and co-evolutionary implications of context-dependent parasitism. *American*
578 *naturalist*, **177**, 510.

579 Vander Wal E, Garant D, Calmé S et al. (2014) Applying evolutionary concepts to
580 wildlife disease ecology and management. *Evolutionary Applications*,
581 10.1111/eva.12168.

582 Vanoverbeke J, De Meester L (2010) Clonal erosion and genetic drift in cyclical
583 parthenogens - the interplay between neutral and selective processes. *Journal of*
584 *Evolutionary Biology*, **23**, 997–1012.

585 Vanoverbeke J, De Gelas K, De Meester L (2007) Habitat size and the genetic
586 structure of a cyclical parthenogen, *Daphnia magna*. *Heredity*, **98**, 419–426.

587 Walker BH (1991) Ecological consequences of atmospheric and climate change.
588 *Climatic Change*, **18**, 301–316.

589 Wolinska J, King KC (2009) Environment can alter selection in host–parasite
590 interactions. *Trends in parasitology*, **25**, 236–244.

591 Wolinska J, Spaak P (2009) The cost of being common: evidence from natural
592 *Daphnia* populations. *Evolution*, **63**, 1893–1901.

593

594 Figure 1. Parasite prevalence over time across 20 replicate mesocosm populations
595 according to (a) mean population temperature and (b) population mixing treatment.
596 The lines represent proportion of hosts infected as predicted by a generalized additive
597 model (GAM; see Table 1) at ambient temperatures of 12°C and 15°C or for each
598 mixing treatment (temperature was fitted as a covariate, but model predictions for two
599 temperatures are shown for clarity). The shaded areas denote 95% confidence
600 intervals (CIs).

601

602 Figure 2. Relationship between epidemic size and (a) mean population temperature,
603 (b) variance in population temperature, and (c) population mixing treatment. Lines
604 show epidemic sizes as predicted by a linear model, shaded areas denote 95% CIs.

605

606 Figure 3. The relative frequencies of each genotype over time in (a) unmixed and (b)
607 mixed populations. There are three sampling points: Start is the beginning of the
608 experiment, when all genotypes were at the same frequency; Pre-epi was on May 24th
609 2015, before epidemics had peaked; and Post-epi was on November 17th 2015, after
610 epidemics had peaked.

611

612 Figure 4. Relationship between host genotypic evenness and (a) epidemic size for pre-
613 epidemic and post-epidemic samples, and (b) time of population sampling for mixed
614 and unmixed populations. Lines show epidemic sizes as predicted by a linear model,
615 shaded areas denote 95% CIs.

616

617 Table 1. **A** Generalized Additive Models fitted to parasite prevalence data. In all four
618 models, sweep volume is fitted as a fixed effect and Julian Day as a non-parametric
619 smoother; mean mesocosm temperature and mixing treatment are fitted as either fixed
620 effects or as modifiers of the Julian Day smoother function. The model that best
621 explains variation in parasite prevalence (here, the model with the lowest AIC value,
622 model 4) is highlighted in bold. **B** Summary analysis for model 4. eDF is the
623 estimated degrees of freedom.

624

625 Table 2. Linear model testing effects of epidemic size, population mixing and
626 sampling time (start, pre-epidemic, post-epidemic) on host genotypic evenness (E_{var} , a
627 measure of host diversity).

628

629

630